Influence of Charge and Ligand on the Finite Temperature Behavior of Gold Clusters: A BOMD Study on Au6 Cluster

ARTICLE *in* THE JOURNAL OF PHYSICAL CHEMISTRY C · SEPTEMBER 2013

Impact Factor: 4.77

3 AUTHORS:

Dar Manzoor
CSIR - National Chemical Laboratory, Pune
7 PUBLICATIONS **15** CITATIONS
SEE PROFILE

Sourav Pal
CSIR - National Chemical Laboratory, Pune
181 PUBLICATIONS **2,836** CITATIONS
SEE PROFILE

Sailaja Krishnamurty
Central Electrochemical Research Institute
54 PUBLICATIONS **893** CITATIONS
SEE PROFILE

THE JOURNAL OF PHYSICAL CHEMISTRY C

Article

pubs.acs.org/JPCC

Influence of Charge and Ligand on the Finite Temperature Behavior of Gold Clusters: A BOMD Study on Au_6 Cluster

Dar Manzoor and Sourav Pal*

Theoretical Chemistry Group, Physical Chemistry Division, CSIR-National Chemical Laboratory, Pune-411 008, India

Sailaja Krishnamurty*

Functional Materials Division, CSIR-Central Electrochemical Research Institute, Karaikudi-630 006, India

Supporting Information

ABSTRACT: Conformation and electronic charge on a gold cluster are known to determine its catalytic property. However, little is known on the finite temperature behavior of various gold cluster conformations. Much less is known on the role of charge or a ligand in stabilizing a conformation at finite temperatures. In this work, we have carried out relativistic density functional theory (DFT) based molecular dynamical simulations on neutral and charged Au_6 clusters with an aim of understanding the stability of ground state conformations as a function of charge on the cluster. Our simulations reveal that cationic and anionic Au_6 clusters undergo conformational transitions at 500 K where as neutral Au_6 cluster retains its ground state conformation up to a temperature of 1100 K. In order to look into the factors leading to the stabilization of neutral Au_6 cluster (or destabilization of cationic and anionic Au_6 clusters), structural and electronic properties are analyzed. Factors such as charge redistribution within the atoms and composition of molecular orbitals are seen to contribute towards stronger Au−Au bonds in Au_6^0 thereby stabilizing it considerably. Following the analysis, simulations are also extended to neutral, cationic, and anionic Au_6−CO_n (n = 1,2) complexes. In the case of CO chemisorbed Au_6 clusters, neutral and negatively charged ground state conformations are stable up to nearly 800 K, while the positively charged Au_6 ground state conformation collapses at room temperature. This work, in short demonstrates how charge or even a ligand can be used to moderate the physical properties of a gold cluster.

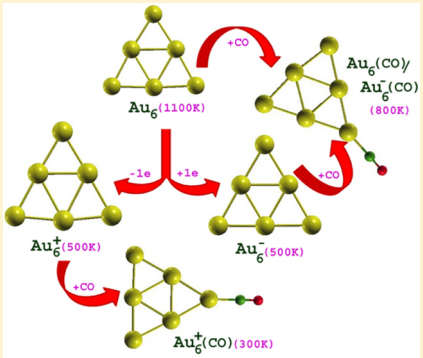

I. INTRODUCTION

Atomic clusters of gold attract a great deal of interest on account of their catalytic,[1−3] electronic,[4,5] magnetic,[6,7] and optical properties.[8,9] The catalytic activity is found to be particularly high in gold clusters with 3 to 55 atoms, also called quantum dots. The extraordinary catalytic activity in this size range is attributed to the quantum confinement of electrons. Hence, presently, there is an impetus for synthesizing small neutral and charged gold clusters in gas phase.[10] Various conformations of Au clusters with 3−20 atoms are now clearly understood owing to the concerted experimental and theoretical studies.[11−17] In one such interesting study,[15] unique configurations were synthesized in gold anionic clusters, for example, hollow cage conformations for Au_{16}^- to Au_{18}^- and a tetrahedral pyramid type conformation for Au_{19}^- and Au_{20}^- In another exciting report, Gruene et al.[16] elucidated the structures of gas phase neutral Au_7, Au_{19} (truncated tetrahedron), and Au_{20} (tetrahedron) clusters using vibrational spectroscopy and density functional based theoretical methods.

The precise knowledge of structures in this size range has motivated several research groups to evaluate their catalytic activity by studying the oxidation of environmentally harmful molecules such as CO.[18−26] These studies reveal a strong dependence of catalytic activity on various factors such as size of the cluster, shape of the cluster, charge on the atomic cluster, support for atomic cluster, mode of synthesis of cluster, and structural fluxionality. For example, recently, Hu et al.[27] have reported that the barrier for oxidation of CO is considerably low for Au_{55}^- as compared to its neutral and positive counterparts. Similarly, in another joint experimental and theoretical work, it is shown that the number of CO molecules that can chemisorb on a gold cluster depends critically on the shape and type of active sites available within a cluster.[28] However, in spite of several attempts by researchers, the dominant factor or even the precise role played by any of the above-mentioned factors in modifying a chemical property is still eluding. What is now clearly understood is that adding or removing even a single electron from a cluster in this size range reorients its catalytic activity dramatically.

Apart from the high rate of activity, a catalytic material is required to be thermally stable at reasonably high operating temperatures. The catalytic applications on large sized Au_n (n >

Received: July 17, 2013
Revised: September 13, 2013
Published: September 16, 2013

   dx.doi.org/10.1021/jp407081m | J. Phys. Chem. C 2013, 117, 20982−20990

200) clusters are generally carried out at subambient (200 K)[1] temperatures, though there are few reports of catalytic reactions on supported nanoclusters between 400 to 1000 K.[29−32] Even in this context, small gold clusters with 3−20 atoms have better advantage as catalytic materials as compared to larger Au nanoparticles due to their higher particle stability.[33−35] The clusters in this size rage reportedly do not suffer from sintering or aggregation effects around room temperature, which are otherwise seen in larger Au nanoparticles. However, there is a possibility of the geometry undergoing some structural transitions at finite temperatures as demonstrated by joint photoelectron spectroscopy (PES) and density functional theory (DFT) based studies on Au_7,[15] Au_{10}^-, and Au_{12}^- clusters.[36,37] Similar conclusions are also drawn on cationic and anionic Au_n ($n \leq 9$) clusters from ion mobility studies at room temperature.[38] In spite of these few attempts, the exact temperatures up to which Au_n (n = 3−20) clusters retain their geometry or oscillate between a few important catalytic conformations (structural fluctuations) is still largely unknown.

In this framework, in one of our recent works,[39] we have noted that Au_6 gas phase conformation remains remarkably stable up to 1100 K. The gold hexamer is a special cluster,[40] with all the three charged states (neutral, anionic and cationic) possessing a D_{3h} planar triangular structure. In its neutral state, the cluster has the largest highest occupied molecular orbital-to-lowest unoccupied molecular orbital (HOMO−LUMO) energy gap (2.13 eV) (more than that of Au_2 cluster which has a gap of 1.97 eV) in the size range of 2−20 atoms and is reportedly aromatic. Another interesting aspect of Au_6 cluster is its unique CO[41] adsorption property. Most of the gold cluster−CO complexes experience a lowering of electron binding energies as compared to the bare gold cluster. In contrast, adsorption of up to 3 CO molecules on Au_6 cluster do not modify the electron binding energies of the complex significantly as compared to the parent Au_6 structure. However, it is its negative counterpart (Au_6^-) that is catalytically very active with an ability to chemisorb up to 6 CO molecules at a given time.[42] Hence, in this work, we attempt to address questions such as (a) Up to what temperature is Au_6^- geometry stable? (b) How does the charge modify the finite temperature behavior of a gold cluster? (c) Does the chemisorption of CO molecule further modify its finite temperature behavior? (d) How do charge-structure−stability-catalytic activity correlate? To answer the above questions, we study the finite temperature behavior of Au_6^- and Au_6^+ clusters and compare it with the behavior of previously studied neutral Au_6. We also extend our study to Au_6-CO_n(n = 1,2) complexes in mono positive, mono negative, and neutral states. The study reveals how ligand chemisorption can play a pivotal role in raising or decreasing the stability temperature of a ground state conformation as compared to its free state. To the best of our understanding, a study attempting to evaluate the role of charge and ligand on the finite temperature behavior or stability of a gold cluster (or rather understanding the charge-structure-catalytic activity-stability pyramid) is so far unavailable in the literature.

II. COMPUTATIONAL DETAILS

All calculations are performed in the framework of Auxiliary Density Functional Theory (ADFT),[43] using a linear combination of Gaussian orbitals as implemented in *deMon2k* code.[44] About 10 conformations are generated for Au_6^- and Au_6^+ clusters. All the conformations are optimized using the Perdew−Burke−Ernzerhof (PBE) exchange and correlation functional[45] with 1997 Stuttgart-Dresden Relativistic Effective Core Potential's (RECP)'s[46] as the basis set for the valence electrons. 5s, 5p, 5d, and 6s electrons are considered to constitute the valence electrons. We note that these ECP's are now documented for accurate prediction of structure as well as spectroscopic properties of Au clusters.[47−49] No additional polarization functions are added. The GEN-A2 auxiliary functions are used to fit the charge density.[50] The convergence of the geometries is based on gradient and displacement criteria with a threshold value of 10^{-5} and the criteria for convergence of SCF cycles is set to 10^{-9}. Following the geometry optimization, harmonic vibrational frequencies are computed for various conformations. All the frequencies were found to be positive for the 10 optimized conformations of Au_6^- and Au_6^+, thereby, indicating them to be a local minima. Analysis of the geometry optimizations reveal that the lowest energy conformation for both Au_6^- and Au_6^+ is a D_{3h} planar triangular structure. This is consistent with the earlier reported ground state geometry for these clusters.[40,41] Au_6-CO_n (n = 1,2) complexes are generated by attaching CO molecules to the cap atoms in Au_6 ground state geometries of all the three states. The geometries of the complexes are optimized using the above-mentioned functional and basis set for Au atoms. The DZVP basis set is used to describe the C and O atoms.

The finite temperature simulations are carried out for lowest energy conformations/optimized complexes using Born−Oppenheimer Molecular Dynamics (BOMD) between 200 to 2000 K. At each temperature, the cluster is equilibrated for a time period of 10 ps followed by a simulation time of 30 ps. The temperature of the cluster is maintained using the Berendsen's thermostat (τ = 0.5 ps) in an NVT ensemble. The nuclear positions are updated using the velocity Verlet algorithm with a time step of 1 fs. We hold the total angular momentum of the cluster to zero, thereby suppressing the cluster rotation.

The atomic positions and bond length fluctuations in the trajectories of Au_6 clusters and Au_6-CO complexes are analyzed using traditional parameters such as δ_{rms} and mean squared ionic displacement (MSD).

δ_{rms} is defined as

$$\delta_{rms} = \frac{2}{N(N-1)} \sum_{i<j} \frac{\sqrt{\langle R_{ij}^2 \rangle_t - \langle R_{ij} \rangle_t^2}}{\langle R_{ij} \rangle_t} \quad (1)$$

where N is the number of particles in the system, R_{ij} is the distance between the ith and jth particle in the system and $<...>_t$ denotes a time average over the entire trajectory. The MSD of an individual atom is defined as

$$\left\langle r_i^2(t) \right\rangle = \frac{1}{NM} \sum_{m=1}^{M} \sum_{l=1}^{N} [R_i(t_{0m} + t) - R_i(t_{0m})]^2 \quad (2)$$

where N is the number of atoms in the system and $R_i(t_{0m})$ is the instantaneous position of atom i at t_0 and $R_i(t_{0m} + t)$ is the corresponding position of atom i after a time interval t. Thus, we average over M different time origins t_{0m} spanning the entire trajectory. The interval between the consecutive t_{0m} for the average is taken to be about 0.0125 ps. The MSD indicates the displacement of atoms in the cluster as a function of time. When the cluster remains in its ground state conformation (i.e., all atoms perform oscillatory motion about fixed positions) the MSD is negligible for individual atoms. On the other hand, when the cluster hops through various conformations, atoms

dx.doi.org/10.1021/jp407081m | J. Phys. Chem. C 2013, 117, 20982−20990

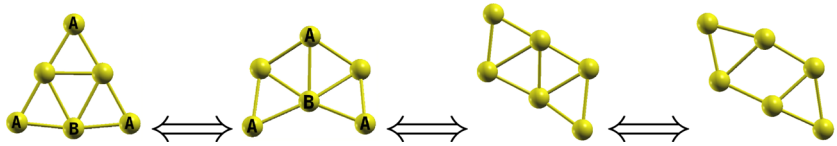

Figure 1. Structural changes observed in Au_6^- between 500 to 800 K.

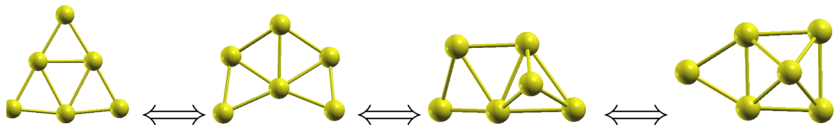

Figure 2. Structural changes observed in Au_6^+ at 500 K.

diffuse through the cluster and the MSD begins to raise. At very high temperatures, when the cluster resembles more like a liquid droplet and does not remain in any conformation for more than 10 fs, the MSD's reach a saturated value of the order of the square of the cluster radius.

III. RESULTS AND DISCUSSION

A. Effect of Finite Temperature on the Behavior of Bare Au Clusters. We begin the discussion on the finite temperature behavior of the Au_6^-, Au_6^+, and Au_6 clusters with an analysis of the ionic motion. Analysis of ionic motion of Au_6^- and Au_6^+ reveals that the atoms in both the clusters vibrate about their equilibrium positions in the ground state geometry up to a temperature of 400 K. Au_6^- undergoes structural transitions between 500 to 800 K. In this temperature range, the cluster transits between various two-dimensional (2D) conformations as seen in Figure 1 before returning back to the ground state. The first three-dimensional (3D) conformation appears around 900 K, and above this temperature the cluster resembles a liquid droplet. Although Au_6^+ also undergoes structural transitions around the same temperature (500 K) as Au_6^-, these structural transitions in Au_6^+ involve both 2D and 3D conformations as shown in the Figure 2. In contrast to the motion of atoms in anionic and cationic Au_6 clusters, the atoms in the neutral cluster vibrate about their mean positions in the ground state geometry up to a temperature of 1100 K.[39] The neutral cluster undergoes structural transformations only above 1100 K before transforming into a liquid droplet around 1600 K. Thus, the Au_6^+ and Au_6^- clusters retain their ground state conformation for much lower temperatures as compared to their neutral counterpart.

This difference in ionic motion of charged gold clusters with respect to that of neutral one is seen clearly from δ_{rms} (Figure 3) and MSD plots (Figure 4). The δ_{rms} for neutral Au_6 is around 0.05 up to a temperature of 1000 K. Around 1200 and 1400 K, the value reaches to 0.08 and 0.1, respectively, which indicates a significant displacement of atoms around 1200 K onward. Beyond 1600 K, the δ_{rms} increases rapidly and reaches a value 0.23 around 2000 K. For both Au_6^+ and Au_6^-, the value of δ_{rms} around 400 K is 0.04 but jumps to a value of Au_6^+ 0.14 and 0.12 around 500 K, respectively. This manifests the onset of structural transformations in these clusters. Above 800 K, the δ_{rms} touches a value close to 0.3 as shown in the Figure 3. This contrasting behavior of structural changes in Au_6^- and Au_6^+ with respect to Au_6 is somewhat weakly seen in MSD plots (see Figure 4). When the atoms vibrate about their equilibrium positions, i.e., around 200 K the MSD plot is similar for all the three clusters. At 600 K, the MSD reaches a value of 1.2 for

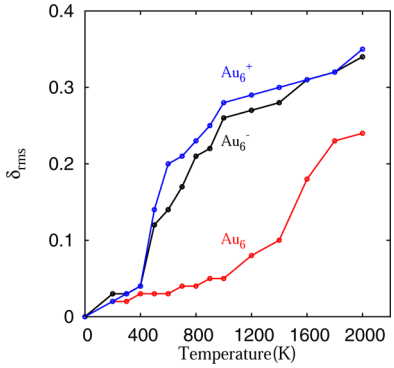

Figure 3. Bond length uctuations (δ_{rms}) as a function of temperature in Au_6, Au_6^-, and Au_6^+.

Au_6^+, where as for Au_6 and Au_6^- it is around 0.1 and 0.3, respectively. The high value of MSD for Au_6^+ at 600 K is indicative of the presence of 3D conformations for this cluster around this temperature. Around 1000 K, the MSD for the cationic and anionic clusters saturate to a value of 2.3, while that of Au_6 is still very low (0.2). Around 1600 K, the MSD's for all the three clusters look somewhat similar (figure not shown).

The ground state geometry of Au_6 being a triangular one, we can attempt to evaluate its reorientation into another conformation by monitoring any of the following distances: (a) distance between a cap atom (called 'A' in Figure 1) and the inner triangular atom (called 'B' in Figure 1), viz., distance 'AB' and/or (b) distance between two cap atoms, viz., distance 'AA' as a function of temperature. The collapse of the triangular structure is characterized by a dramatic increase or decrease in either of these bond distances or both. Shown in Figure 5 are the A−A and A−B interatomic distances for Au_6^- cluster at 400 and 600 K. At 600 K, both these inter atomic distances undergo a dramatic shift owing to the structural changes from the triangular structure to the next conformation shown in Figure 1. In contrast, it can be seen from Figure 5 that A−B inter atomic distances in Au_6 at 1000 K fluctuate around the same average value as that of 400 K albeit with higher amplitude. Similar observation is also noted for A−A inter atomic distances of Au_6 cluster between 400 and 1000 K (Figure not shown).

Thus, the analysis of ionic motion, δ_{rms}, MSD's and critical inter atomic distances clearly demonstrate that among the three clusters, the neutral Au_6 remains in its ground state conformation up to 1100 K while its charged counterparts do not remain in the ground state conformation beyond 400 K.

dx.doi.org/10.1021/jp407081m | J. Phys. Chem. C 2013, 117, 20982−20990

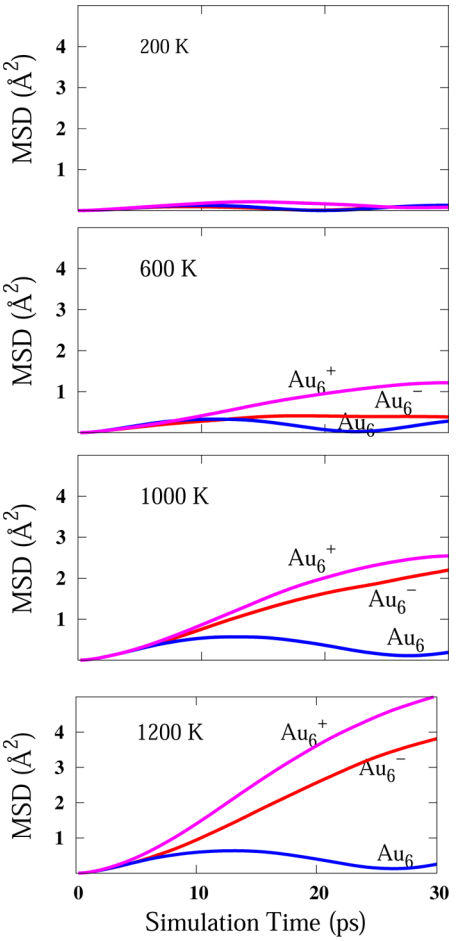

Figure 4. MSD of atoms in Au_6, Au_6^-, and Au_6^+ clusters between 200 to 1200 K.

Incidentally, 1100 K is very close to the melting temperature of bulk gold (1337 K).

Usually in clusters the surface-to-volume ratio is higher as compared to that of bulk. This is traditionally expected to bring down the temperature up to which the solid cluster is stable (as compared to that of bulk). However, this traditional expectation is seen to be inconsistent in case of some unique sized Na,[51] Ga,[52] and Al.[53] Later studies revealed that the structural and electronic properties contribute considerably towards these variations.[54] In the case of gold, among most of the small sized neutral clusters, only Au_4, Au_6, and Au_{10} have been found to remain in their ground state beyond 500 K. Au_6 is the most stable one of these three (1100 K as compared to 800 of Au_4 and Au_{10}). This stability is lost upon adding or removing an electron to Au_6.

In order to bring out the factors stabilizing the neutral Au_6 conformation (or factors destabilizing the charged Au_6 conformations), we analyze their structural and electronic properties. Figure 6 shows the detailed structural properties of Au_6 in all the three states. The six atoms in each conformation can be classified into two types depending on their distinct chemical environment, viz., (a) 'B' atoms forming an inner triangle and (b) 'A' atoms capping the edge of each inner triangle. In the neutral cluster, the inner triangle ('B−B−B' triangle) is an equilateral one with an inter atomic distance of 2.84 Å. The outer triangles (ABB) have a 'A−B−B' angle of 57.5° and a 'B−A−B' angle of 64° (and hence, the outer

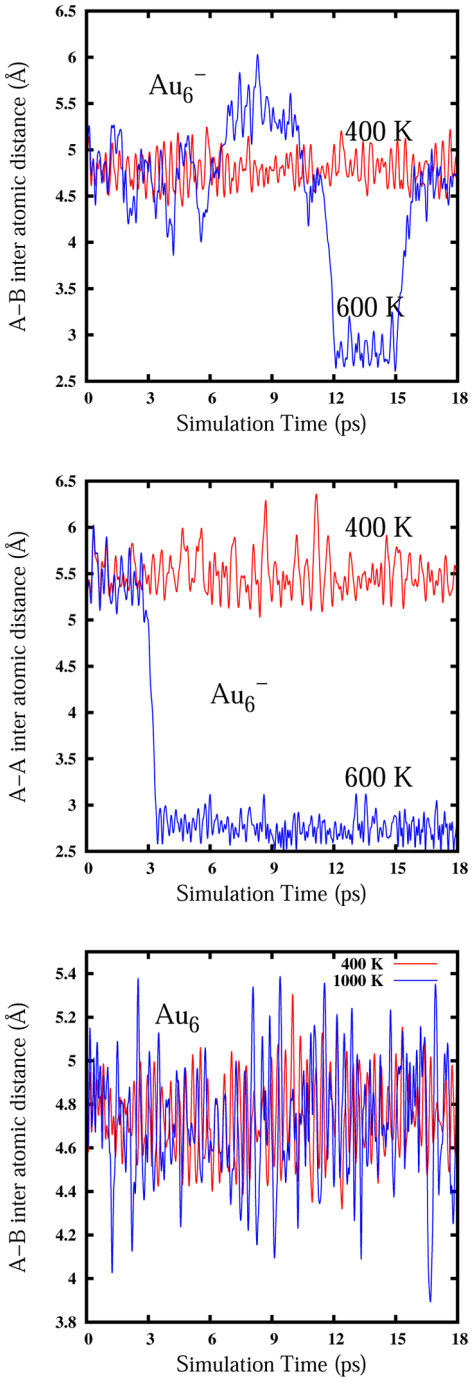

Figure 5. Fluctuation in the A−B and A−A inter atomic distances (refer to Figure 1) within Au_6^- and Au_6 clusters at various temperatures.

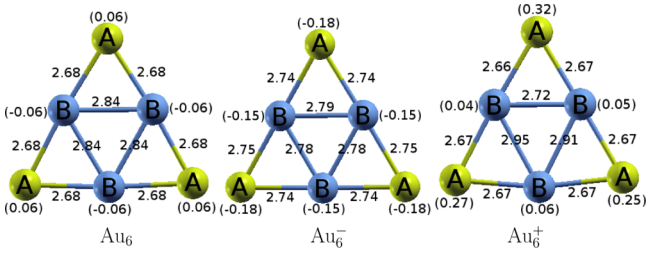

Figure 6. Structural details of Au_6, Au_6^-, and Au_6^+ clusters.

dx.doi.org/10.1021/jp407081m | J. Phys. Chem. C 2013, 117, 20982−20990

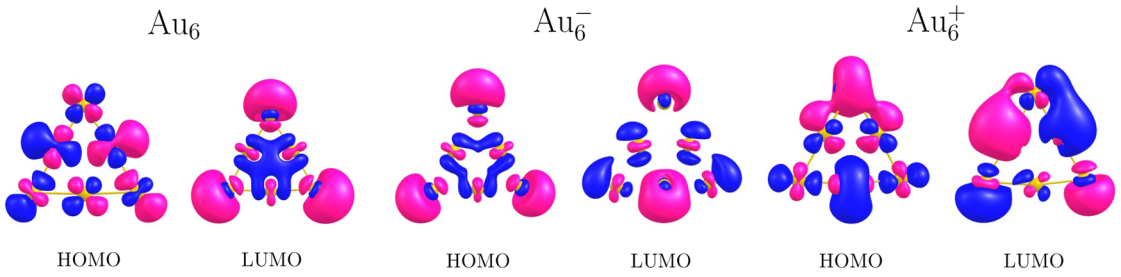

Figure 7. HOMO and LUMO molecular orbitals of Au_6, Au_6^- and Au_6^+ clusters. The red and the blue lobes represent the positive and negative sign of the wave function.

triangles are not equilateral). These structural features reflect in the NBO[55,56] (natural bond orbital) charge distribution within the cluster. The inner triangle atoms (B) are negatively charged (each atom has −0.06 electrons on it), whereas the cap atoms (A) are positively charged (each having a positive charge of 0.06). Consequently, there is a net transfer of nearly 0.20 electrons from the cap atoms to the inner triangular atoms leading to larger 'B−B' bonds lengths (larger by 0.15 Å) as compared to the 'A−B' interatomic distances.

In the case of Au_6^-, the 'B−B' inter atomic distances decrease to a value of 2.78 Å as compared to the neutral one. The 'A−B' inter atomic distances increase to a value of 2.76 Å leading to nearly equivalent 'A−B' and 'B−B' inter atomic distances. However, the entire cluster expands on the whole as compared to the neutral conformation to fit in the extra electron as seen from the values of the area of triangle. The area of the negatively charged cluster is about 13.13 Å as compared to 12.65 Å of neutral cluster. The net charge difference between all the 'A' and all the 'B' atoms in the negatively charged cluster is 0.09 electrons. The 'A' atoms have a negative charge of −0.18, and 'B' atoms have a negative charge of −0.15. Thus, the extra electron is shared by both 'A' and 'B' atoms with the cap atoms having an excess of 0.03 electrons each. However, it is important to note that this excess 0.03 electrons is localized on each atom, unlike in case of neutral cluster where the excess of 0.06 electrons on each inner triangular atom can contribute to a delocalized electron cloud of 0.20 electrons. Owing to this nearly equivalent charge distribution in all the six sites in Au_6^-, it is able to accommodate up to 6 CO molecules as seen in one of the earlier studies, albeit with structural modifications for the fourth CO molecule.[42] In case of Au_6^+, two 'A' atoms lie out of plane with respect to the rest of the atoms in the cluster (resulting in 'A−B−A' angles to be 168.9°) indicating that the cluster is not perfectly planar to start with. The 'B−B' inter atomic distances in this case are 2.95 Å, 2.91 Å, and 2.72 Å, respectively. Thus, the inner triangle in Au_6^+ is no longer equilateral unlike its negative and neutral counterparts. Deviation from the symmetry reflects in the atomic charge distribution where all the cap atoms no longer carry equivalent charges. The two 'A' atoms lying out of plane have an atomic charges of 0.25 and 0.27 as compared to 0.32 on the third 'A' atom. A net positive charge of 0.84 is localized on the cap atoms ('A' atoms), while a net positive charge of 0.15 is on the inner triangle atoms ('B' atoms).

Figure 7 shows the frontier molecular orbitals of Au_6, Au_6^-, and Au_6^+ clusters. The HOMO of neutral Au_6 cluster shows s−d hybridization with 37% s and 63% d character On the other hand, the HOMO's of anionic and cationic Au_6 clusters are predominantly s (71%) and d type (78%), respectively. Thus, the s−d hybridization is some what more higher in the neutral cluster as compared to the negative one. The s−d hybridization is least in cationic cluster among the three. The HOMO LUMO gap of the Au_6 cluster is 2.13 eV, whereas for the Au_6^- and Au_6^+ clusters it is 0.34 and 0.14 eV, respectively. Also interestingly, Au_6^- with relatively greater s−d hybridization (and HOMO−LUMO energy gap) with respect to Au_6^+ undergoes a 2d−3d structural transition only around 900 K as compared to the cationic one at 500 K. In some of the reports recently,[38,57] it is proposed that enhanced s−d hybridization (which is due to relativistic effects) is responsible for higher stabilization of planar gold clusters. Thus, we note that (i) enhanced s−d hybridization, (ii) higher HOMO−LUMO energy gap, and (iii) the presence of a negatively charged inner triangle atoms bonded to positively charged caps jointly contribute to the higher stability of Au_6^0 as compared to Au_6^- and Au_6^+.

Finally, in order to have a complete picture of stabilizing/destabilizing factors in each cluster, we elaborate on the movements of individual atoms within the cluster. The δ_{rms} for 'A−B'(cap-inner triangular bond length fluctuations) and 'B−B' (inner triangular-inner triangular bond length fluctuations) bond lengths for all the three clusters at 400 K are shown in Figure 8. The reason for choosing 400 K is that at this temperature all the three clusters oscillate around their ground

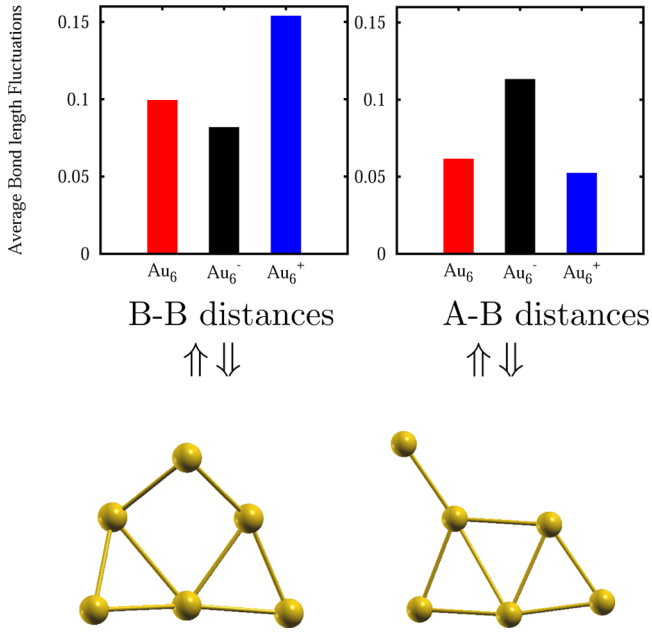

Figure 8. Averaged bond length uctuations in 'A−B' and 'B−B' atom pairs in Au_6, Au_6^- and Au_6^+ clusters. Also given below are the conformations seen in Au_6^+ and Au_6^-respectively at 500 K before the ground state transitsinto another conformation.

dx.doi.org/10.1021/jp407081m | J. Phys. Chem. C 2013, 117, 20982−20990

state. An analysis of the individual atom movements at this temperature is expected to bring about an understanding of the atoms that catalyze the structural modifications in each cluster. Figure 8 shows that the 'A−B' bond distances fluctuations are larger in Au_6^-. In other words, the cap atoms have higher atomic displacements in the negatively charged cluster as compared to the neutral and positive clusters. On the other hand, in the case of Au_6^+, it is the inner triangular atoms that move considerably. This is consistent with the type of conformations that we note in the ionic motions around 500 K. Around 500 K, it is the cap atoms in Au_6^- that get displaced first leading to other type of conformations. On the other hand, in the case of Au_6^+, it is the inner triangular atomic motions that catalyze the transition into other high energy conformations. In contrast, Au_6, with higher s−d hybridization, has low 'A−B' and 'B−B' bond length fluctuations. The absence of any catalyzing atomic movements allows the cluster to retain its conformation up to to much higher temperatures as compared to its charged counterparts.

B. Effect of Finite Temperature on CO Adsorbed Au Clusters. Chemical reaction of gold clusters with CO ligand is one of the most studied issues by both experimental and theoretical methods. Hence, there is a considerable amount of understanding available on the electronic and structural properties of CO adsorbed gold clusters.[41,42,58,59] However, very little is known on the influence of CO adsorption towards the finite temperature behavior of gold clusters. Hence, we complete this study by addressing the finite temperature behavior of CO molecule adsorbed Au_6 clusters. For this purpose, one and two CO molecules are adsorbed respectively on neutral, cationic and anionic Au_6 clusters and finite temperature simulations carried out on the complexes as mentioned earlier. Our study reveals that CO ligated neutral Au_6 clusters remain stable up to 800 K as compared to the 1100 K of bare (nonligated) cluster. Until 800 K, the only structural changes observed in Au_6-CO_n (n = 1,2) complexes are the rotation of Au−Au−C−O bonds between 0 and 180 degrees. The fact that the complexes retains their original conformation up to this temperature is demonstrated using average bond length fluctuations in Figure 9. Around 1000 K, both the complexes undergo structural transitions to 3D conformations. The conformational change is driven by the motion of the CO bonded Au atom moving out of the plane of other 5 Au atoms along with the CO ligand. In the case of the Au_6-CO_2 complex, only one of the CO bonded Au atom moves out of the plane of the rest the complex. The CO molecule/s remains bonded to the same Au atom up to a temperature of 1400 K, beyond which it dissociates itself from the Au cluster. In summary, the neutral Au_6 CO ligated conformations are about 300 K less stable than the bare Au_6 conformation. On the other hand, the ligated anionic D3h conformations remain stable up to 800 K as compared to 500 K in bare anionic cluster. Thus, the stability of ligated neutral clusters decreases by 300 K while that of ligated anionic clusters increases by 300 K. The ligated cationic Au_6 conformations do not retain their D_{3h} conformation even at 300 K by undergoing structural transitions into other 2D and 3D structures. Factors contributing to the modification of the finite temperature behavior of Au_6 clusters when complexed with CO molecule/s are elaborated below.

Figure 10 shows the atomic nomenclature used for CO adsorbed complexes. The CO ligated cap atoms are named 'A1', and the unligated cap atoms are called 'A'. Similarly, the inner triangular atoms bonded to 'A1' are called 'B1'. Figure 10 also

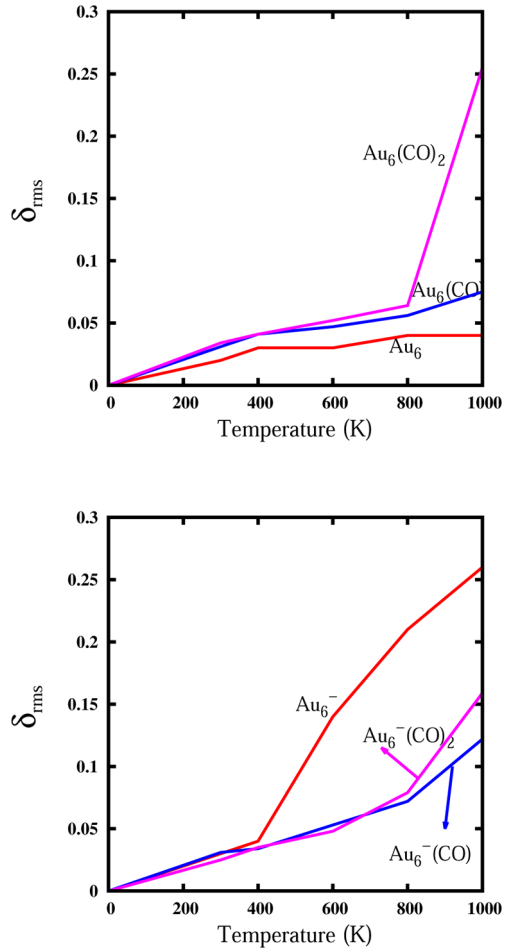

Figure 9. Bond length uctuations (δ_{rms}) as a function of temperature in Au_6-$(CO)_n$ and $Au_6^-(CO)_n$ complexes where n = 0, 1, 2.

gives the differential bond lengths in all the three clusters with respect to the bare clusters, which shows that upon CO molecule adsorption, specific pockets of cluster undergo major structural modifications. In the case of neutral Au_6-CO_n complexes, the overall structural modification that can be seen is shrinking of bond lengths between inner triangular atoms and the elongation of outer triangular bond lengths. A similar trend is also noted in $Au_6^+(CO)_n$ complexes. In the case of $Au_6^-(CO)_n$ complexes, the outer triangle is seen to shrink while the inner triangle is seen to increase in size. Significant CO bond elongations are seen in the $Au_6^-(CO)_n$ complexes (the bare CO bond distance is 1.14 Å), indicating a strong Au_6^- cluster−CO molecule interaction.

Analysis of MOs for all the complexes reveals that in the case of a neutral cluster, the HOMO orbital is not affected while the LUMO orbital is modified as compared to the bare cluster (see Supporting Information). This leads to a reduction of the HOMO−LUMO energy gap in both the CO adsorbed Au_6^0 clusters (energy gap is 1.77 and 1.34 for CO = 1 and 2, respectively). In the case of charged complexes, HOMO and LUMO orbitals are both modified significantly. As a consequence, the HOMO−LUMO energy gap in negatively charged complexes increases to 0.46 and 0.52, respectively. The energy gap in the $Au_6^+(CO)_n$ complexes is 0.12 and 0.10, respectively. Most importantly, the contribution of 6S and 5D orbitals towards the HOMO and LUMO do not change

dx.doi.org/10.1021/jp407081m | J. Phys. Chem. C 2013, 117, 20982−20990

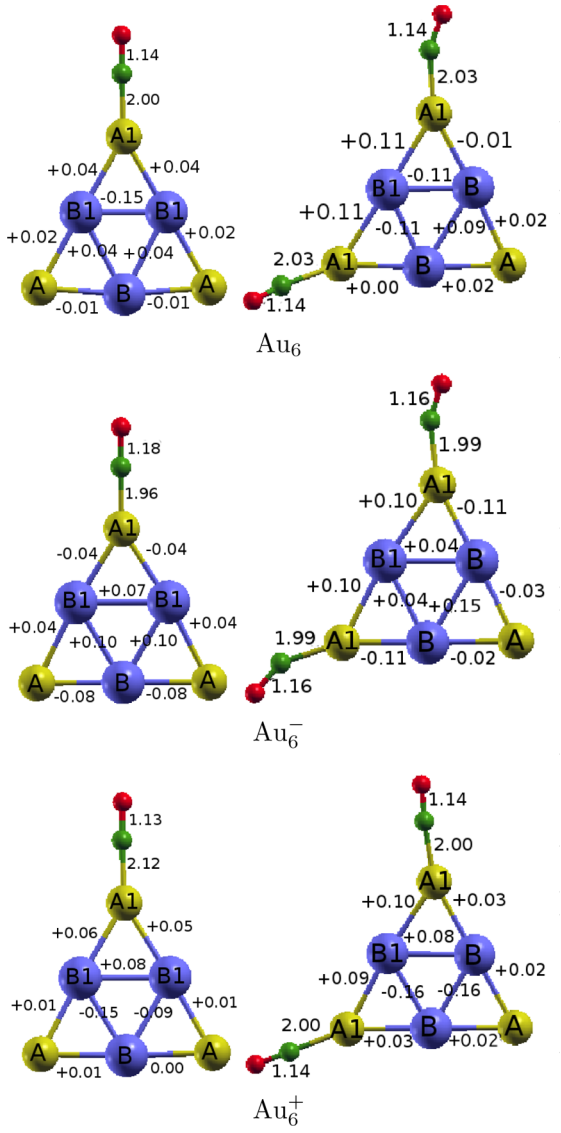

Figure 10. Differential structural parameters for Au_6-$(CO)_n$, Au_6^- $(CO)_n$, and Au_6^+ $(CO)_n$ complexes where n = 1, 2 with respect to Au_6, Au_6^-, and Au_6^+ clusters, respectively.

significantly as compared to the bare cluster in all the three cases.

The cluster−ligand interaction and the resulting stability (destability) of gold cluster is understood by evaluating the atomic charge distribution within all the complexes. Table 1 shows the atomic charge distribution within neutral, cationic, and anionic (Au_6−CO_n (n = 0,1,2)) complexes. It is seen that in the case of neutral and positively charged clusters, the CO molecule acts as a reducing agent and looses some electrons to the cluster. In the case of neutral clusters, the gold cluster gains 0.10 and 0.14 e, respectively, upon adsorption of one and two CO molecule, s which is also seen from the increase in the C−O stretching frequency to 2168 cm^{-1} (stretching frequency for free CO is 2133 cm^{-1}). In the positively charged cluster, the gold cluster gains 0.21 and 0.39 e, respectively. The interacting cap atoms ('A1' atoms) in both these cases are most positively charged. These cap atoms attempt to move out of the plane in an attempt to share the electrons distributed over rest of the cluster. Hence, the CO ligated neutral and positively charged Au_6 clusters are less stable as compared to their bare

Table 1. Atomic Charges for $Au_6(CO)_n$ (n = 0,1,2) Complexes (cf. Figure 3 and Figure 7) As Obtained by Natural Bond Orbital Analysis

Atom	Au_6	Au_6−$(CO)_1$	Au_6−$(CO)_2$
atom 'A1'	–	0.068	0.061
atom 'A'	0.06	−0.013	−0.055
atom 'B1'	–	−0.049	−0.003
atom 'B'	−0.06	−0.043	−0.101
carbon	–	0.458	0.439
oxygen	–	−0.359	−0.369
charge on CO	–	0.099	0.140
Atom	Au_6^-	Au_6^-−$(CO)_1$	Au_6^-−$(CO)_2$
atom 'A1'	–	−0.059	−0.030
atom 'A'	−0.18	−0.171	−0.193
atom 'B1'	–	−0.194	−0.171
atom 'B'	−0.15	−0.122	−0.194
carbon	–	0.357	0.350
oxygen	–	−0.449	−0.445
charge on CO	–	−0.092	−0.190
Atom	Au_6^+	Au_6^+−$(CO)_1$	Au_6^+−$(CO)_2$
atom 'A1'	–	0.195	0.177
atom 'A'	0.32, 0.25, 0.27	0.192	0.106
atom 'B1'	–	0.064	0.044
atom 'B'	0.06, 0.05, 0.04	0.086	0.055
carbon	–	0.495	0.490
oxygen	–	−0.288	−0.296
charge on CO	–	0.210	0.388

counterparts. On the other hand, in the case of a negatively charged cluster, each CO molecule gains about 0.091 e. Interestingly, in this case, the interacting Au atom looses more than 0.1 electrons. Thus, analysis of charge and HOMO orbitals of $Au_6^-(CO)_n$ (n = 1,2) (see Supporting Information) indicates that there is charge transfer from cluster to the anti bonding orbital of CO molecule, which is further reflected from the decrease in the C−O stretching frequency (1955 cm^{-1}) as compared to the free CO. This charge transfer stabilizes the negatively charged cluster. As a consequence, the A−B inter atomic bond length fluctuations (cf. Figure 8 and the Supporting Information) that catalyze the transition from the ground state geometry to the next high energy conformation is reduced considerably, thereby stabilizing the anionic clusters by an additional 300 K.

IV. CONCLUSIONS

In conclusion, our BOMD simulations shed light on the effect of charge and ligand on the finite temperature behavior of the Au_6 cluster. The present study reflects how adding or removing an electron from a cluster has contrasting effect on its thermodynamic stability coupled with the structural and electronic properties. The finite temperature behavior indicates that neutral Au_6 is stable up to much higher temperature, 1100 K, compared to the cationic and anionic Au_6 clusters (500 K each). Further, ligating the cluster with a small probe such as CO can also moderate the finite temperature behavior. Thus, the present study demonstrates that charge or ligand can be used for fine-tuning not only the chemical but also physical properties of gold clusters, there by affecting their potential use in applications at various temperatures.

dx.doi.org/10.1021/jp407081m | J. Phys. Chem. C 2013, 117, 20982−20990

■ ASSOCIATED CONTENT

Supporting Information

Figures showing the frontier molecular orbitals of $Au_6(CO)_n$ and $Au_6^-(CO)_n$ where n = 1 and average bond length fluctuations in $Au_6^-(CO)_n$ complexes where n = 0, 2. This material is available free of charge via the Internet at http://pubs.acs.org.

■ AUTHOR INFORMATION

Corresponding Authors

*E-mail: sailaja.raaj@gmail.com.
*E-mail: s.pal@ncl.res.in.

Notes

The authors declare no competing financial interest.

■ ACKNOWLEDGMENTS

The authors acknowledge the Center of Excellence in Computational Chemistry (COESC) at CSIR-NCL, Pune for the calculations presented and CSIR XIIth 5-year plan for Multiscale simulation of materials (MSM) project grant. D.M. acknowledges University Grants Commision (UGC), India for Senior Research Fellowship and S. Das and Mudit Dixit for special discussions. S.P. acknowledges a grant from the SSB project of CSIR and the J. C. Bose Fellowship project of DST towards partial completion of the work.

■ REFERENCES

(1) Haruta, M.; Yamada, N.; Kobayashi, T.; Iijima, S. Gold catalysts prepared by coprecipitation for low-temperature oxidation of hydrogen and of carbon monoxide. *J. Catal.* **1989**, *115*, 301−309.
(2) Hashmi, A. S. K. Homogeneous Gold Catalysts and Alkynes: A Successful Liaison. *Gold Bull.* **2003**, *36*, 3−9.
(3) Haruta, M. Size and support-dependency in the catalysis of gold. *Catal. Today.* **1997**, *36*, 153−166.
(4) Jing-Xin, Y.; Xiang-Rong, C.; Stefano, S.; Cheng, Y. Quantum transport of Au−S−S−Au nanoscale junctions. *Appl. Phys. Lett.* **2012**, *100*, 013113−013117.
(5) Torma, V.; Vidoni, O.; Simon, U.; Schmid, G. Charge Transfer Mechanisms between Gold Clusters. *Eur. J. Inorg. Chem.* **2003**, *2003*, 1121−1127.
(6) Li, X.; Kiran, B.; Cui, Li-Feng.; Wang, L.-S. Magnetic Properties in Transition-Metal-Doped Gold Clusters: M@Au6 (M = Ti,V,Cr). *Phys. Rev. Lett.* **2005**, *95*, 253401.
(7) Pundlik, S. S.; Kalyanaraman, K.; Waghmare, U. V. First Principle Investigation of the Atomic and Electronic Structure and Magnetic Moments in Gold Nanoclusters. *J. Phys. Chem. C* **2011**, *115*, 3809−3820.
(8) Sánchez-Castillo, A.; Noguez, C.; Garzoán, I. L. On the Origin of the Optical Activity Displayed by Chiral-Ligand-Protected Metallic Nanoclusters. *J. Am. Chem. Soc.* **2010**, *132*, 1504−1505.
(9) Gautier, C.; Bürgi, T. Chiral *N*-Isobutyryl-cysteine Protected Gold Nanoparticles: Preparation, Size Selection, and Optical Activity in the UV−vis and Infrared. *J. Am. Chem. Soc.* **2006**, *128*, 11079−11087.
(10) Maity, P.; Xie, S.; Yamauchi, M.; Tsukuda, T. Stabilized gold clusters: From isolation toward controlled synthesis. *Nanoscale* **2012**, *4*, 4027−4037.
(11) Gilb, S.; Weis, P.; Furche, F.; Ahlrichs, R.; Kappes, M. M. Structures of small gold cluster cations Au_n^+ (n < 14): Ion mobility measurements versus density functional calculations. *J. Chem. Phys.* **2002**, *116*, 4094−4101.
(12) Lechtken, A.; Neiss, C.; Kappes, M. M.; Schooss, D. Structure determination of gold clusters by trapped ion electron diffraction: Au_{14}^-, Au_{19}^-. *Phys. Chem. Chem. Phys.* **2009**, *11*, 4344−4350.
(13) Häkkinen, H.; Yoon, B.; Landman, U.; Li, X.; Zhai, H. J.; Wang, L. S. On the Electronic and Atomic Structure of Small Au_N^- (N = 4−14) Clusters: A Photoelectron Spectroscopy and Density Functional Study. *J. Phys. Chem. A* **2003**, *107*, 6168−6175.
(14) Zhu, M.; Christine, M. A.; Frederick, J. H.; George, C. S.; Rongchao, J. Correlating the Crystal Structure of A Thiol Protected Au_{25} Cluster and Optical Properties. *J. Am. Chem. Soc.* **2008**, *130*, 5883−5885.
(15) Bulusu, S.; Li, X.; Wang, L.-S.; Zeng, X. C. Evidence of hollow golden cages. *Proc. Natl. Acad. Sci. U.S.A.* **2006**, *103*, 8326−8330.
(16) Gruene, P.; Rayner, D. M.; Redlich, B.; van der Meer, A. F. G.; Lyon, J. T.; Meijer, G.; Fielicke, A. Structures of Neutral Au_7, Au_{19}, and Au_{20} Clusters in the Gas Phase. *Science* **2008**, *321*, 674−676.
(17) Wang, L.-M.; Wang, L.-S. Probing the electronic properties and structural evolution of anionic gold clusters in gas phase. *Nanoscale* **2012**, *4*, 4038−4053.
(18) Zhang, C.; Yoon, B.; Landman, U. Predicted Oxidation of CO Catalyzed by Au Nanoclusters on a Thin Defect-Free MgO Film Supported on a Mo(100) Surface. *J. Am. Chem. Soc.* **2007**, *129*, 2228−2229.
(19) Jena, N K.; Chandrakumar, K. R. S.; Ghosh, S. K. DNA Base-Gold Nanocluster Complex as a Potential Catalyzing Agent: An Attractive Route for CO Oxidation Process. *J. Phys. Chem. C* **2012**, *116*, 17063−17069.
(20) Lopez, N.; Nørskov, J. K. Catalytic CO Oxidation by Gold Nanoparticle: A Density Functional Study. *J. Am. Chem. Soc.* **2002**, *124*, 11262−11263.
(21) Yoon, B.; Häkkinen, H.; Landman, U.; Wörz, A.; Antonietti, J.; Abbet, S.; Judai, K.; Heiz, U. Charging Effects on Bonding and Catalyzed Oxidation of CO on Au_8 Clusters on MgO. *Science* **2005**, *307*, 403−407.
(22) Gao, Y.; Pei, Y.; Chen, Z.; Zeng, X. Catalytic Activities of Subnanometer Gold Clusters (Au_{16}−Au_{18}, Au_{20} and Au_{27}−Au_{35}) for CO Oxidation. *ACS Nano* **2011**, *5*, 7818−7829.
(23) Socaciu, L.; Hagen, J.; Bernhardt, T.; Wöste, L.; Heiz, U.; Häkkinen, H.; Landman, U. Catalytic CO Oxidation by Free Au_2^-: Experiment and Theory. *J. Am. Chem. Soc.* **2003**, *125*, 10437−10445.
(24) Häkkinen, H.; Landman, U. Gas-Phase Catalytic Oxidation of CO by Au_2^-. *J. Am. Chem. Soc.* **2001**, *123*, 9704−9705.
(25) Bürgel, C.; Reilly, N. M.; Johnson, G. E.; Mitric, R.; Kimble, M. L.; Castleman, A. W., Jr.; Bonačić-Koutecký, V. Influence of Charge State on the Mechanism of CO Oxidation on Gold Clusters. *J. Am. Chem. Soc.* **2008**, *130*, 1694−1698.
(26) Yoon, B.; Häkkinen, H.; Landman, U. Interaction of O_2 with Gold Clusters: Molecular and Dissociative Adsorption. *J. Phys. Chem. A* **2003**, *107*, 4066−4071.
(27) Tang, D.; Hu, C. DFT Insight into CO Oxidation Catalyzed by Gold Nanoclusters: Charge Effect and Multi-State Reactivity. *J. Phys. Chem. Lett.* **2011**, *2*, 2972−2977.
(28) Zhai, H. J.; Wang, L. S. Chemisorption sites of CO on small gold clusters and transitions from chemisorption to physisorption. *J. Chem. Phys.* **2005**, *122*, 051101−051104.
(29) Veith, G. M.; Lupini, A. R.; Rashkeev, S.; Pennycook, S. J.; Mullins, D. R.; Schwartz, V.; Bridges, C. A.; Dudney, N. J. Thermal stability and catalytic activity of gold nanoparticles supported on silica. *J. Catal.* **2009**, *262*, 92−101.
(30) Lopez-Sanchez, J. A.; Dimitratos, N.; Hammond, C.; Brett, G. L.; Kesavan, L.; White, S.; Miedziak, P.; Tiruvalam, R.; Jenkins, R. L.; Carley, A. F.; et al. Facile removal of stabilizer ligands from supported gold nanoparticles. *Nat. Chem.* **2011**, *3*, 551−556.
(31) Menarda, L. D.; Xu, F.; Nuzzo, R. G.; Yang, J. C. Preparation of TiO_2 supported Au nanoparticle catalysts from a Au_{13} cluster precursor: Ligand removal using ozone exposure versus a rapid thermal treatment. *J. Catal.* **2006**, *243*, 64−73.
(32) Maciejewski, M.; Fabrizioli, P.; Grunwaldt, J.-D.; Becker, O. S.; Baiker, A. Supported gold catalysts for CO oxidation: Effect of calcination on structure, adsorption and catalytic behaviour. *Phys. Chem. Chem. Phys.* **2001**, *3*, 3846−3855.
(33) Haruta, M. Catalysis of Gold Nanoparticles Deposited on Metal Oxides. *CATTECH* **2002**, *6*, 102−115.

(34) Haruta, M. When Gold Is Not Noble: Catalysis by Nanoparticles. *Chem. Rec.* **2003**, *3*, 75−85.
(35) Haruta, M. Gold as a novel catalyst in the 21st century: Preparation, working mechanism and applications. *Gold Bull.* **2004**, *37*, 27−36.
(36) Huang, W.; Wang, L.-S. Probing the 2D to 3D Structural Transition in Gold Cluster Anions Using Argon Tagging. *Phys. Rev. Lett.* **2009**, *102*, 153401−153404.
(37) Wang, L.-M.; Pal, R.; Huang, W.; Zeng, X. C.; Wang, L.-S. Observation of earlier two-to-three dimensional structural transition in gold cluster anions by isoelectronic substitution: MAu_n^- (n = 8−11; M = Ag,Cu). *J. Chem. Phys.* **2010**, *132*, 114306−114314.
(38) Schooss, D.; Weis, P.; Hampe, O.; Kappes, M. M. Determinig the size-dependent structure of ligand-free gold-cluster ions. *Phil. Trans. R. Soc. A* **2010**, *368*, 1211−1243.
(39) De, H. S.; Krishnamurty, S.; Mishra, D.; Pal, S. Finite Temperature Behavior of Gas Phase Neutral Au_n (n = 3−10) Clusters: A First Principles Investigation. *J. Phys. Chem. C* **2011**, *115*, 17278−17285.
(40) Taylor, K. J.; Jin, C.; Conceicao, J.; Wang, L. S.; Cheshnovsky, O.; Johnson, B. R.; Norlander, P. J.; Smalley, R. E. Vibrational autodetachment spectroscopy of Au_6^-: Image-charge-bound states of gold ring. *J. Chem. Phys.* **1990**, *93*, 7515−7519.
(41) Zhai, H.-J.; Dai, B.; Kiran, B.; Li, J.; Wang, L.-S. Unique CO Chemisorption Properties of Gold Hexamer: $Au_6(CO)_n^-$ (n = 0−3). *J. Am. Chem. Soc.* **2005**, *127*, 12098−12106.
(42) Zhai, H.-J.; Pan, L.-L.; Dai, B.; Kiran, B.; Li, J.; Wang, L.-S. Chemisorption-induced Structural Changes and Transition from Chemisorption to Physisorption in $Au_6(CO)_n^-$ (n = 4−9). *J. Phys. Chem. C* **2008**, *112*, 11920−11928.
(43) Köster, A. M.; Reveles, J. U.; del Campo, J. M. Calculation of exchange-correlation potentials with auxiliary function densities. *J. Chem. Phys.* **2004**, *121*, 3417−3424.
(44) Koster, A. M.; Calaminici, P.; Casida, M. E.; F-Moreno, R.; Geudtner, G.; Goursot, A.; Heine, T.; Ipatov, A.; Janetzko, F.; del Campo, J. M.; Patchkovskii, S.; Reveles, J. U.; Vela, A.; Salahub, D. R. *deMon2k*; The deMon Developers: Cinvestav, Mexico City, 2006.
(45) Perdew, J. P.; Burke, K.; Ernzerhof, M. Generalized Gradient Approximation Made Simple. *Phys. Rev. Lett.* **1996**, *77*, 3865−3868.
(46) Schwerdtfeger, P.; Dolg, M.; Schwarz, W. H. E.; Bowmaker, G. A.; Boyd, B. W. D. Relativistic effects in gold chemistry. I. Diatomic gold compounds. *J. Chem. Phys.* **1989**, *91*, 1762−1774.
(47) Dolg, M. In *Modern Methods and Algorithms of Quantum Chemistry*; Grotendorst, J., Ed.; NIC Series; John von Neumann Institute for Computing: Jülich, Germany, 2000; Vol. *1*, p 479.
(48) De, H. S.; Krishnamurty, S.; Pal, S. Density Functional Investigation of Relativistic Effects on the Structure and Reactivity of Tetrahedral Gold Clusters. *J. Phys. Chem. C* **2009**, *113*, 7101−7106.
(49) De, H. S.; Krishnamurty, S.; Pal, S. Understanding the Reactivity Properties of Au_n ($6 < n < 13$) Clusters Using Density Functional Theory Based Reactivity Descripters. *J. Phys. Chem. C* **2010**, *114*, 6690−6703.
(50) Calaminici, P.; Janetzko, F.; Köster, A. M.; Mejia-Olvera, R.; Zuniga-Gutierrez, B. Density functional theory optimized basis sets for gradient corrected functionals: 3d transition metal systems. *J. Chem. Phys.* **2007**, *126*, 044108−044118.
(51) Schmidt, M.; Kusche, R.; Kronmüller, W.; von Issendorff, B.; Haberland, H. Experimental Determination of the Melting Point and Heat Capacity for a Free Cluster of 139 Sodium Atoms. *Phys. Rev. Lett.* **1997**, *79*, 99102.
(52) Breaux, G. A.; Hillman, D. A.; Neal, C. M.; Benirschke, R. C.; Jarrold, M. F. Gallium Cluster Magic Melters. *J. Am. Chem. Soc.* **2004**, *126*, 8628−8629.
(53) Breaux, G. A.; Neal, C. M.; Cao, B.; Jarrold, M. F. Melting, Premelting, and Structural Transitions in Size-Selected Aluminum Clusters with around 55 Atoms. *Phys. Rev. Lett.* **2005**, *94*, 173401−173404.
(54) Chacko, S.; Joshi, K.; Kanhere, D. G.; Blundell, S. A. Why do gallium clusters have a higher melting point than the bulk? *Phys. Rev. Lett.* **2004**, *92*, 135506−135510.
(55) Single point calculations for calculating NBO charges are done using Gaussian 09.
(56) Frisch, M. J.; Trucks, G. W.; Schlegel, H. B.; Scuseria, G. E.; Robb, M. A.; Cheeseman, J. R.; Scalmani, G.; Barone, V.; Mennucci, B.; Petersson, G. A.; Nakatsuji, H.; Caricato, M.; Li, X.; Hratchian, H. P.; Izmaylov, A. F.; Bloino, J.; Zheng, G.; Sonnenberg, J. L.; Hada, M.; Ehara, M.; Toyota, K.; Fukuda, R.; Hasegawa, J.; Ishida, M.; Nakajima, T.; Honda, Y.; Kitao, O.; Nakai, H.; Vreven, T.; Montgomery, J. A., Jr.; Peralta, P. E.; Ogliaro, F.; Bearpark, M.; Heyd, J. J.; Brothers, E.; Kudin, K. N.; Staroverov, V. N.; Kobayashi, R.; Normand, J.; Raghavachari, K.; Rendell, A.; Burant, J. C.; Iyengar, S. S.; Tomasi, J.; Cossi, M.; Rega, N.; Millam, N. J.; Klene, M.; Knox, J. E.; Cross, J. B.; Bakken, V.; Adamo, C.; Jaramillo, J.; Gomperts, R.; Stratmann, R. E.; Yazyev, O.; Austin, A. J.; Cammi, R.; Pomelli, C.; Ochterski, J. W.; Martin, R. L.; Morokuma, K.; Zakrzewski, V. G.; Voth, G. A.; Salvador, P.; Dannenberg, J. J.; Dapprich, S.; Daniels, A. D.; Farkas, Ö.; Ortiz, J. V.; Cioslowski, J.; Fox, D. J. *Gaussian 09*, revision A.1; Gaussian, Inc.: Wallingford, CT, 2009.
(57) Häkkinen, H.; Moseler, M.; Landman, U. Bonding in Cu, Ag, and Au Clusters: Reletivistic Effects, Trends, and Surprises. *Phys. Rev. Lett.* **2002**, *89*, 033401−033404.
(58) Jena, N. K.; Chandrakumar, K. R. S.; Ghosh, S. K. Theoretical Investigation on the Structure and Electronic Properties of Hydrogen and Alkali-Metal-Doped Gold Clusters and Their Interaction with CO: Enhanced Reactivity of Hydrogen-Doped Gold Clusters. *J. Phys. Chem. C* **2009**, *113*, 17885−17892.
(59) Pal, R.; Huang, W.; Wang, Y.-L.; Hu, H.-S.; Bulusu, S.; Xiong, X.-G.; Li, J.; Wang, L.-S.; Zeng, X. C. Chemisorption-induced 2D−3D−2D structural transitions in Gold Heptamer: $(CO)_nAu_7^-$ (n = 1−4). *J. Phys. Chem. Lett.* **2011**, *2*, 2288−2293.